The Irminger Gyre: Circulation, convection, and interannual variability

K. Våge[1,7], R.S. Pickart[1], A. Sarafanov[2], Ø. Knutsen[3], H. Mercier[4], P. Lherminier[4], M. Bersch[5], H. van Aken[6], J. Meincke[5], and D. Quadfasel[5]

(1) Woods Hole Oceanographic Institution, Woods Hole, USA, (2) P.P. Shirshov Institute of Oceanology, Moscow, Russia, (3) SINTEF Fisheries and Aquaculture, Trondheim, Norway, (4) Laboratoire de Physique des Océans, Plouzané, France, (5) Institut für Meereskunde, Universität Hamburg, Hamburg, Germany, (6) Royal Netherlands Institute for Sea Research, Den Burg, Netherlands, (7) Now at Geophysical Institute, University of Bergen, Bergen, Norway.

Introduction

The Irminger Gyre (IG) is a recirculation gyre in the western Irminger Sea, east of southern Greenland (Figure 1). It is a central feature of the western subpolar gyre and potentially important to deep convection in the Irminger Sea leading to the formation of Labrador Sea Water (LSW). A second site of LSW formation outside of the Labrador Basin would have important consequences for our understanding of the North Atlantic Meridional Overturning Circulation, the modification of the dense overflow waters from the Nordic seas, and the stratification and ventilation of the interior North Atlantic.

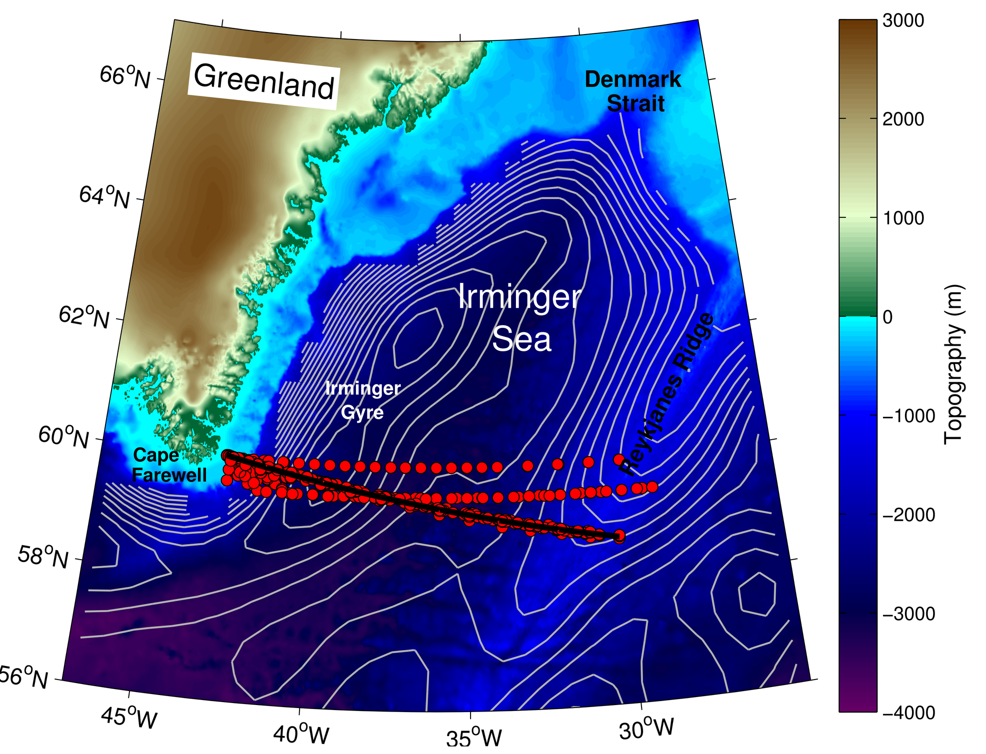

Figure 1: Topography of southeast Greenland and the Irminger Sea from the Etopo2 2-minute elevation data base. The red circles mark the locations of hydrographic stations and the black line identifies the AR7E least squares regression line onto which all in-situ data have been projected. The gray lines are contours of objectively mapped geostrophic pressure at 700 *db*, from Lavender et al. [2000]. The closed contours in the western Irminger Sea reveal the location of the Irminger Gyre.

Our main objectives in this study are to (i) quantify the structure, transport and interannual variability of the Irminger Gyre and (ii) investigate the importance of the Irminger Sea as a source region for LSW.

Data and methods

- 32 hydrographic transects between 1991 and 2007 were projected onto the AR7E line (Figure 1) and interpolated onto a standard grid.
- 47 direct velocity (ADCP) transects between 1999 and 2002 were used as reference to construct absolute geostrophic velocity sections for that period.
- Validated by good agreement with the ADCP-referenced velocities, absolute geostrophic velocity sections for the full period were constructed using satellite altimetry as reference.
- Velocities exceeding ± 2 cm/s may in general be considered significant for any pentadal or longer average.

References

Häkkinen, S., Rhines, P. B., 2004. Decline of subpolar North Atlantic circulation during the 1990s. Science 304, 555–559.

Lavender, K. L., Davis, R. E., Owens, W. B., 2000. Mid-depth recirculation observed in the interior Labrador and Irminger Seas by direct velocity measurements. Nature 407, 66–69.

Pickart, R. S., Straneo, F., Moore, G. W. K., 2003. Is Labrador Sea Water formed in the Irminger Basin? Deep Sea Research I 50, 23–52.

Contact information: kjetil@whoi.edu

Mean state

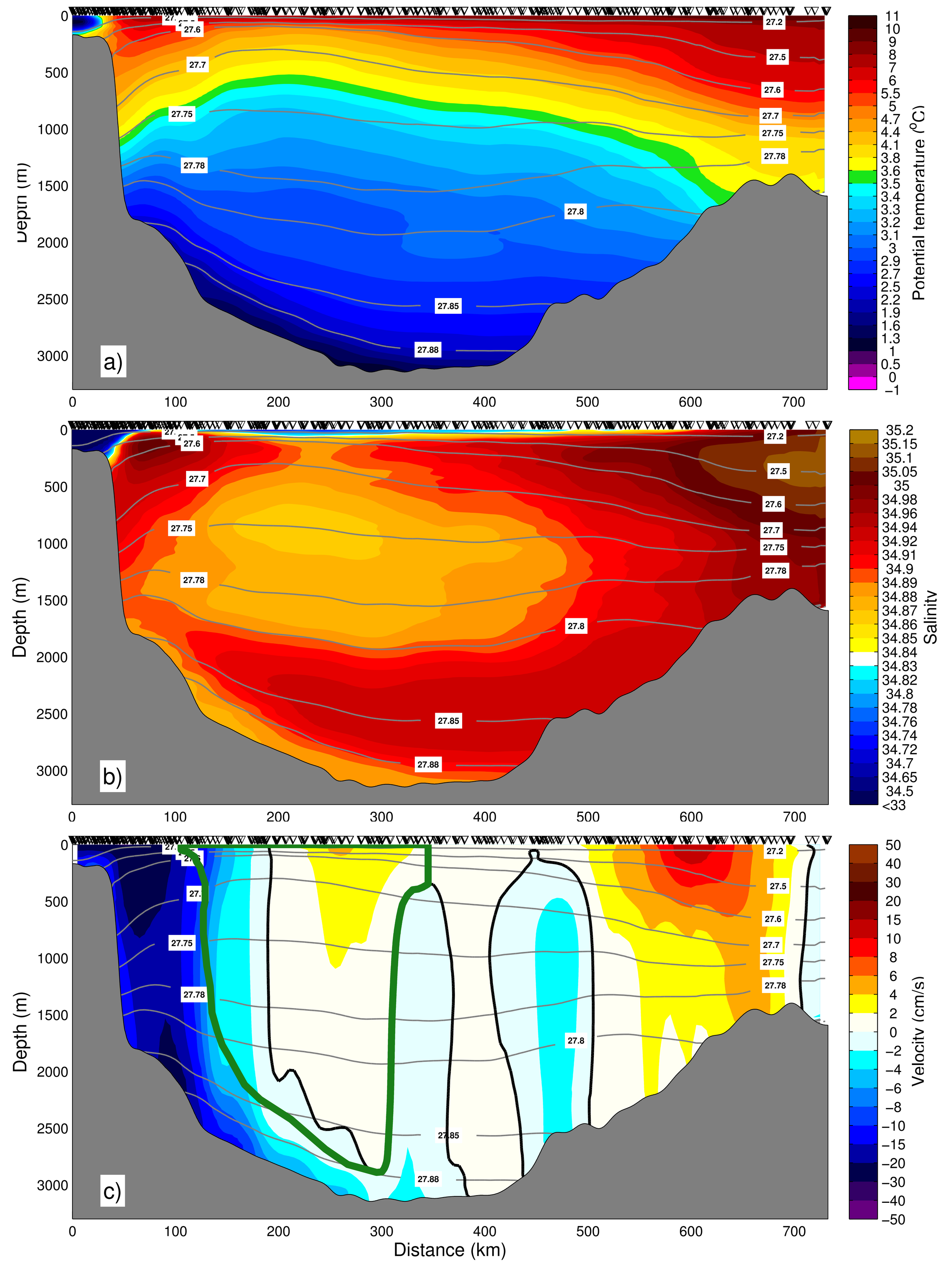

Figure 2: Vertical sections of **a)** potential temperature (°C), **b)** salinity, and **c)** absolute geostrophic velocity (positive to the northeast, cm/s) averaged over the period 1991-2007. The grey lines are potential density contours, and the black and green lines in **c)** are the zero velocity contour and the IG boundary, respectively. The black triangles mark station locations.

Transport

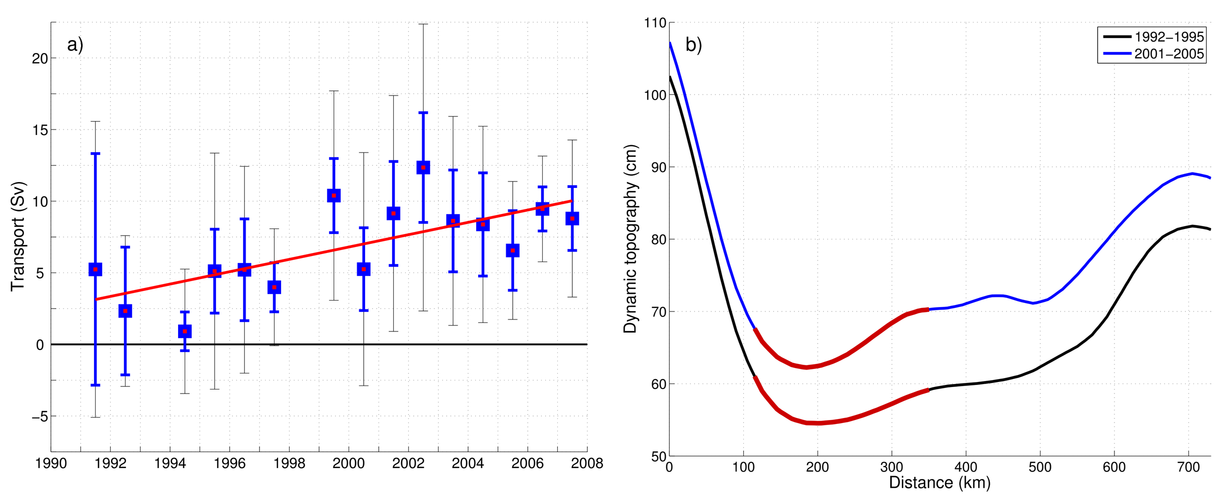

Figure 3: **a)** Irminger Gyre transport (Sv). The black error bars indicate the total error, while the blue error bars show the altimeter standard error only. The red line is the least squares best fit through the data. **b)** Altimeter dynamic topography (cm) along AR7E for the early 1990s and the early 2000s. The approximate width of the IG is indicated by the red segment.

Interannual variability

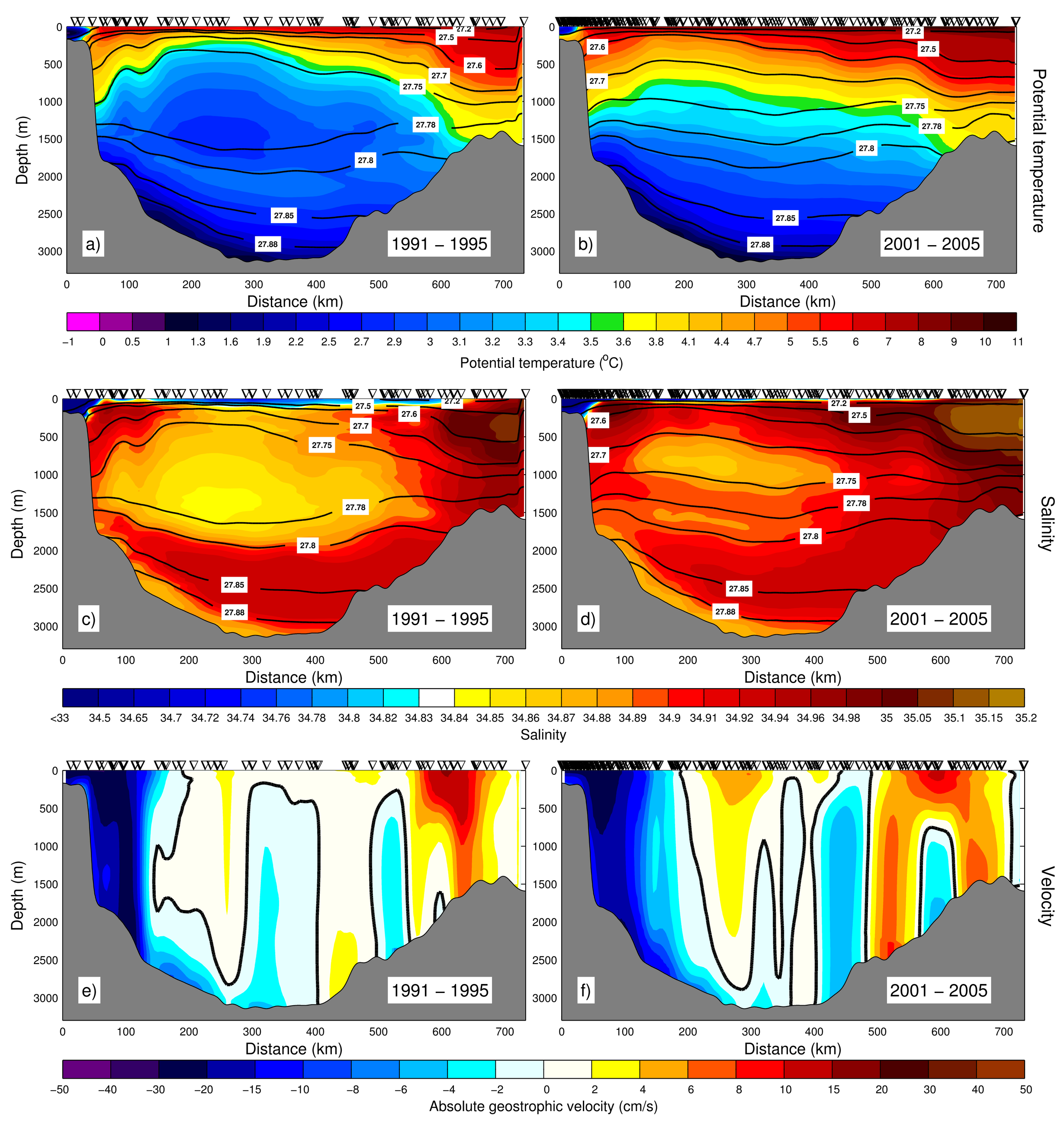

Figure 4: Vertical sections of **a, b)** potential temperature (°C), **c, d)** salinity, and **e, f)** absolutely referenced geostrophic velocity (cm/s) averaged over the periods **a, c, e)** 1991-1995 and **b, d, f)** 2001-2005. The black contours are potential density or zero velocity, and the black triangles indicate station locations.

The Irminger Gyre is outlined by the thick green line in Figure 2c. Its mean transport was 6.8 ± 1.8 Sv. Surprisingly the IG transport increased through the period of observations (1991-2007, Figures 3a and 4e, f) despite a reduction in the wind stress and buoyancy components of the atmospheric forcing. This is likely due to a non-uniform restratification that led to a steepening of the sea surface height gradient in the central Irminger Sea (Figure 3b).

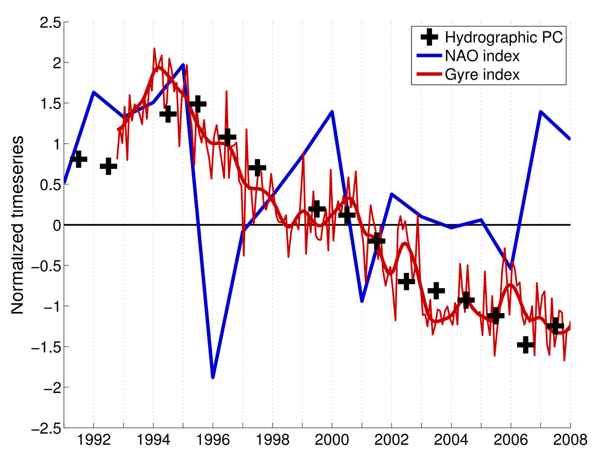

Figure 5: Principal components timeseries of the first empirical orthogonal function (EOF) mode computed from annual mean hydrographic data (potential temperature, salinity, and potential vorticity) within the Irminger Gyre. The blue and red timeseries are the NAO index and the gyre index of Häkkinen and Rhines [2004], respectively.

The dominant intermediate water mass is LSW, identifiable by low salinity and weak stratification (Figure 2a, b). Significant changes have taken place in concert with the changing atmospheric conditions represented by the NAO index. Severe winters with high convective activity resulted in a voluminous dome of lower LSW in the first pentad of the 1990s (Figure 4a, c). Milder winters followed, and by the first pentad of the 2000s there was only a trace remaining of the lower LSW, while a layer of upper LSW had appeared at shallower depths (Figure 4b, d). Note the high level of agreement between the EOF principal components timeseries and the gyre index (Figure 5).

Convection

It has been argued that LSW can be formed in the southwest Irminger Sea in addition to the Labrador Sea [Pickart et al., 2003]. To elucidate the issue of local versus remote ventilation, we use a volumetric T-S approach. We expect that arrival of LSW from the Labrador Sea will present an unmistakable signal, and find evidence that deep convection did occur in the Irminger Sea during the early 1990s.

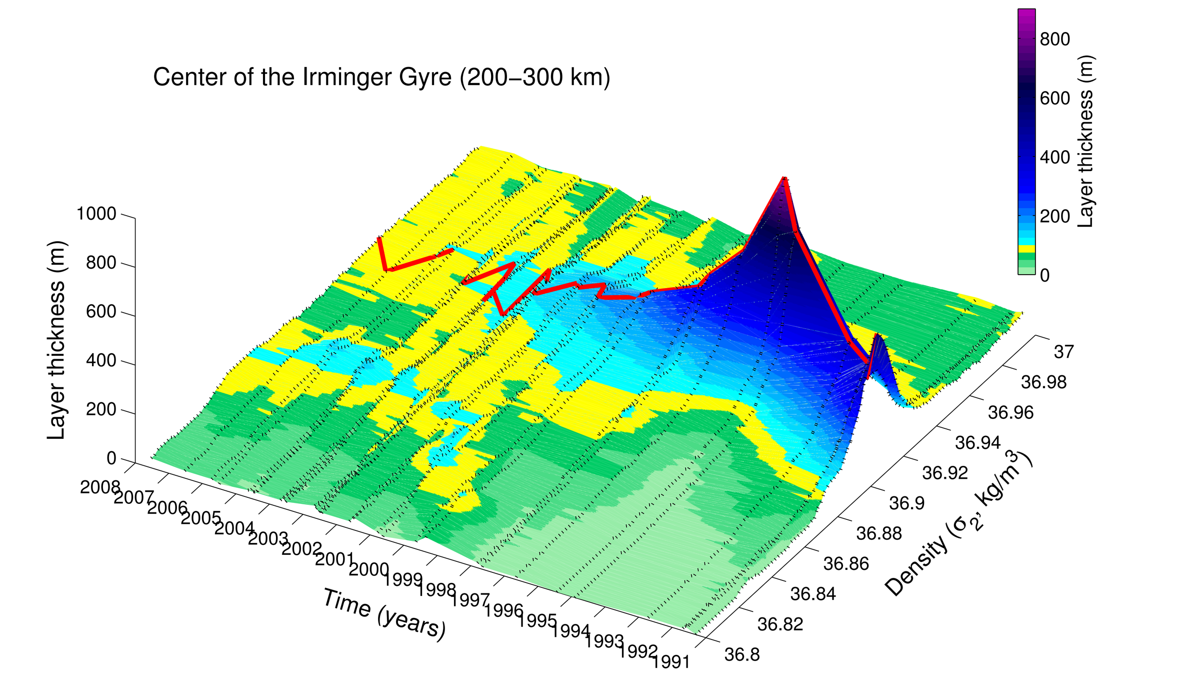

Figure 6: Average thickness (m) of potential density layers within the Irminger Gyre (200-300 km along AR7E) in relation to potential density ($\sigma_2, kg/m^3$) of the given layer and time (years). The vertical extent of each overlapping layer was 0.01 kg/m^3, and individual layers were separated by 0.002 kg/m^3. The red line follows the crest of the thickness ridge and hence identifies the lower LSW core in each section. The dashed lines indicate when individual sections were occupied.

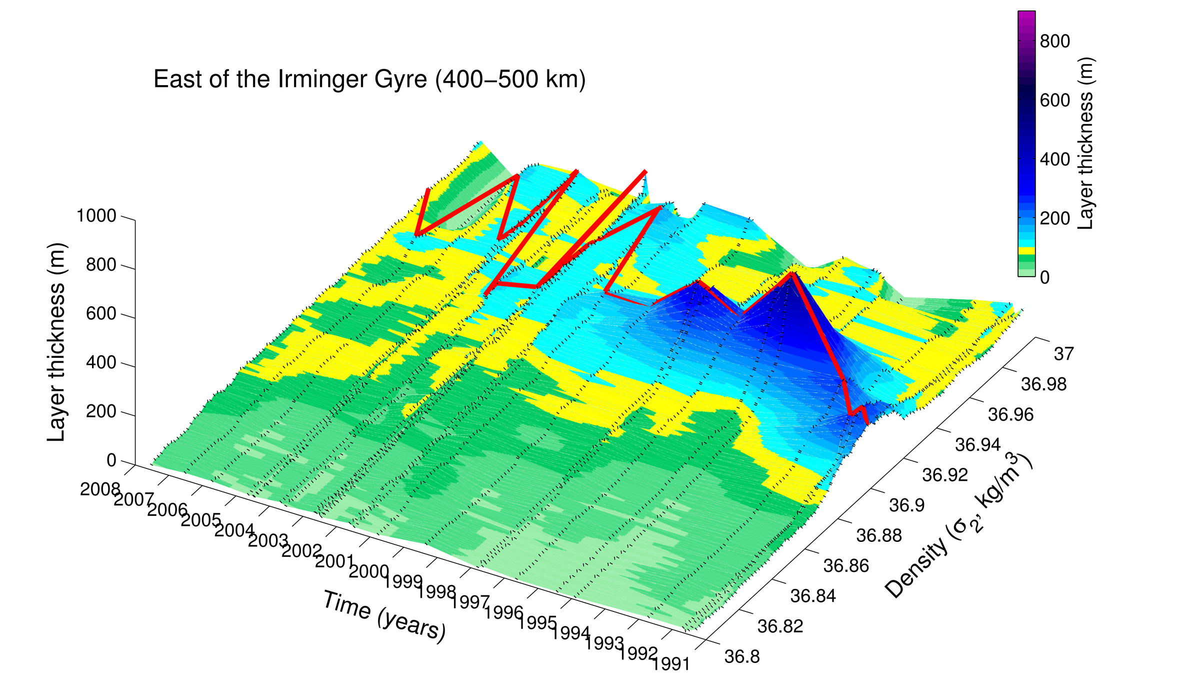

Figure 7: As Figure 6, but for the region east of the IG between 400 and 500 km along AR7E.

Inside of the Irminger Gyre there was a single peak of lower LSW in 1995 (Figure 6), too early to be a remote signal from the maximum convection year in the Labrador Sea (1994). However, outside of the gyre there were two maxima (Figure 7). The timing and properties of the latter peak are only reconcilable with a remote Labrador Sea source, and consistent as well with the velocity field.

Conclusions

- The mean transport of the Irminger Gyre was 6.8 ± 1.8 Sv, and over the 17-year study period the transport increased at a rate of 4.3 Sv per decade.
- The LSW layer thickness' temporal evolution suggests that local convection formed lower LSW during the early 1990s within the Irminger Gyre.